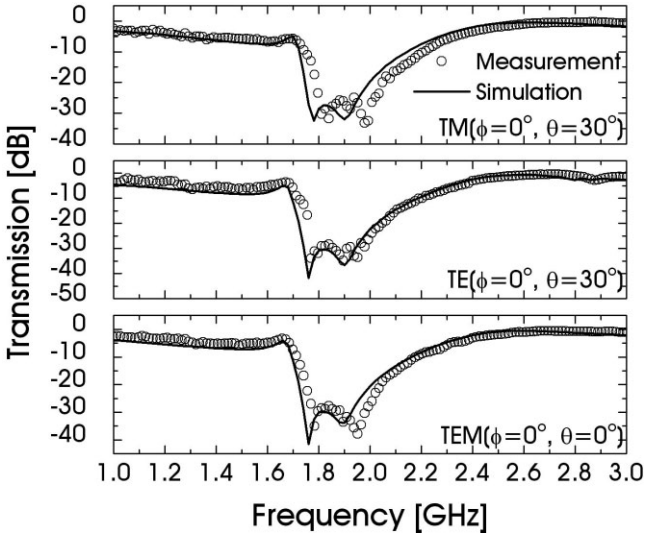

Figure 5 Transmission characteristics of the double-layer FSS for the normal and inclined incidences

As the distance h increases, stop bandwidths correspond to the larger attenuation value increase rather slowly compare to those of the smaller attenuation values. From the analysis results shown in Figures 3 and 4, we have determined that the optimum spacing between double-layer FSS is 5 mm, which can effectively lower the center frequency of stop band and enlarge the stop bandwidth, simultaneously. The predicted and measured transmission behaviors for the finally designed double-layer FSS are given in Figure 5 and Table 1. In the figure, both normal and inclined ($\varphi = 0°$, $\theta = 30°$) incidences are considered. As can be seen from Figure 5, both the uplink and downlink bands can be blocked with our double-layer FSS with 30-dB attenuation, which is impossible with the single-layer FSS.

Moreover, by cascading the two identical FSS layers with optimum spacing, we can obtain about three times wider stop band with sharper roll-off characteristic compared to the single-layer case. Although there are slight frequency shifts, the predicted and the measured results show good agreement for both cases, and this validates that the proposed broadband FSS is insensitive to angular variation, which is a crucial property required for the spatial filter.

3. CONCLUSIONS

We have proposed a broadband spatial band-stop filter using Sierpinski space-filling curve (SSG) operating at Korean PCS communication band. We have first designed a single-layer FSS consisting of SSG of iteration Level 4 but its stop band is somewhat narrow to cover the whole target band. To increase the bandwidth of the stop band, two SSG FSS layers are stacked with some gap in-between. Consequently, the fabricated band-stop filter with double-layer SSG FSS has a 20-dB attenuation bandwidth over 255 MHz both for normal and inclined incidences, which is very wide enough to cover the whole PCS band.

REFERENCES

1. R. Mittra, C.H. Chan, and T. Cwik, Technique for analyzing frequency selective surfaces-a review, IEEE Proc 76 (1988), 1593–1615.
2. B.A. Munk, Frequency selective surface: Theory and design, Wiley-Interscience, New York, NY, 2000.
3. E.A. Parker and A.N.A. El Sheikh, Convoluted array elements and reduced size unit cells for frequency-selective surfaces, IEE Proc 138 (1991), 19–22.
4. J. McVay, N. Engheta, and A. Hoorfar, High impedance metamaterial surfaces using Hilbert-curve inclustons, IEEE Microwave Wireless Compon Lett 14 (2004), 130–132.
5. H. Sagan, Space-filling curves, Springer-Verlag, Berlin, Germany, 1994.

COMPACT SIX-BAND INTERNAL ANTENNA WITH STACKED PERIODIC-GROOVED PLANES

Kyung K. Kang, Jae W. Lee, Choon Sik Cho, and Taek K. Lee
School of Electronics, Telecommunication and Computer Engineering, Korea Aerospace University, 100 Hanggongdae-Gil, Hwajon-Dong, Deogyang-Gu, Gyeonggi-Do 412-791, Korea; Corresponding author: jwlee1@kau.ac.kr

Received 26 February 2008

ABSTRACT: *This article deals with a design of compact six-band internal antenna using two identically stacked periodic-grooved patches and shorting plates and covering the frequency bands composed of cellular (824–894 MHz), GSM (880–960 MHz), DCS (1710–1880 MHz), PCS (1850–1990 MHz), UMTS (1920–2170 MHz), and ISM (2400–2480 MHz) under the criteria −7.3 dB for the first five bands and −6 dB for the last band, respectively. To accomplish this goal, the planar inverted-F antenna (PIFA) with periodic grooves is suggested, analyzed, and verified by using two commercially available softwares, CST MWS and HFSS based on the FDTD and FEM algorithms, respectively, and carrying out the measurements in terms of return loss, radiation patterns, and gains.* © 2008 Wiley Periodicals, Inc. Microwave Opt Technol Lett 50: 2718–2722, 2008; Published online in Wiley InterScience (www.interscience.wiley.com). DOI 10.1002/mop.23776

Key words: *internal antenna; periodic grooves; multi-band antennas*

1. INTRODUCTION

Thanks to the remarkable developments of mobile communication systems, as the wireless and portable devices are applied in many areas and situations. Especially, the recent trends required for hand-held devices are small size, light weight, omnidirectional radiation pattern, higher gain, and wide impedance bandwidth to provide multifunction/band behaviors.

To satisfy the general requirements of antenna (size, efficiency, bandwidth, etc.), many researchers have investigated the design method of internal multiband antennas [1]. As a candidate for internal antenna, PIFA is introduced with the advantages of easy fabrication and flexibility for various packaging structures [2].

In this article, it is shown that the narrow bandwidth as a demerit of PIFA can be overcome by changing the pattern of the ground plane, the mutual coupling level between the shorting plates, and the distance between two identical radiation patches resulting in additional resonant frequency and improving antenna performances at the upper frequency band [1–3].

2. ANTENNA CONFIGURATION

The general antenna (Internal Antenna) structure is shown in Figure 1 with two identically stacked periodic-grooved radiation-patches, feeding post, shorting plates in parallel, and slotted ground planes. The detailed descriptions for radiating patches and shorting plates are listed and marked in Table 1 and Figures 1(b)–1(d). The periodic-grooved slits are continuously inserted on each patch and result in the lower resonant frequency by making the total current path longer [4]. In our simulation and measurement, the shape and size of two patches are almost the same as those shown in Figures 1(b) and 1(c) except the length parameter, p15.

As an important point of the proposed antenna, the area, g5 multiplied by g6, of the ground plane near the resonating patch is removed and slotted to control the resonant frequency and to enhance the antenna input impedance bandwidth. In addition, an improvement of the bandwidth in return-loss point of view has been accomplished by setting the gap, s3, between two

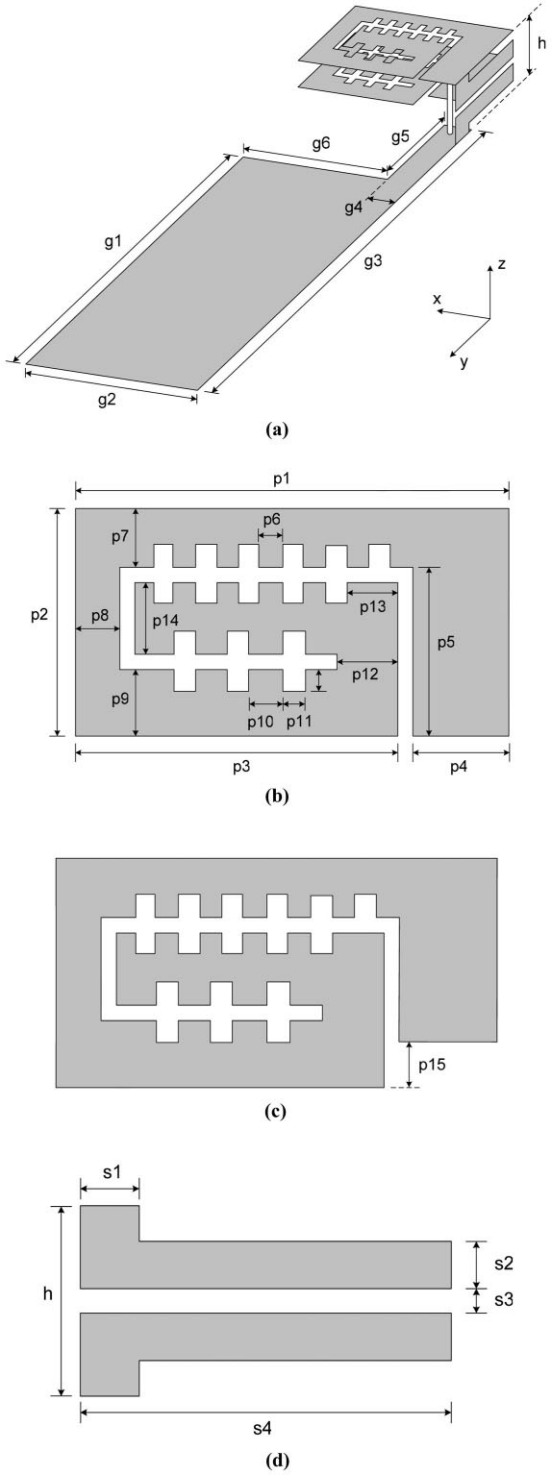

Figure 1 Proposed antenna geometry (a) side view, (b) main patch, (c) sub patch, and (d) shorting plates

TABLE 1 Optimized Parameter Values of the Proposed Antenna

Parameter	Value (mm)
g1	84
g2	32
g3	103
g4	5
g5	19
g6	27
p1	30
p2	15
p3	22.25
p4	6.75
p5	11.5
p6	1.5
p7	4
p8	3
p9	4.5
p10	2.25
p11	1.5
p12	4.25
p13	3.5
p14	4.5
p15	3
s1	2.5
s2	2
s3	1
s4	15
h	8

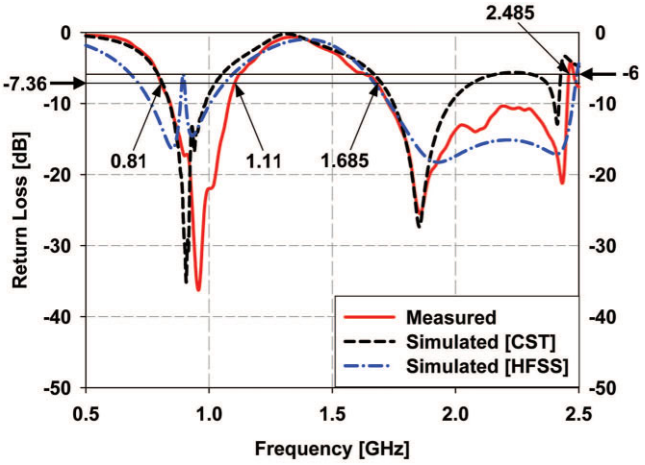

Figure 2 Comparison of the simulated and measured return losses. [Color figure can be viewed in the online issue, which is available at www.interscience.wiley.com]

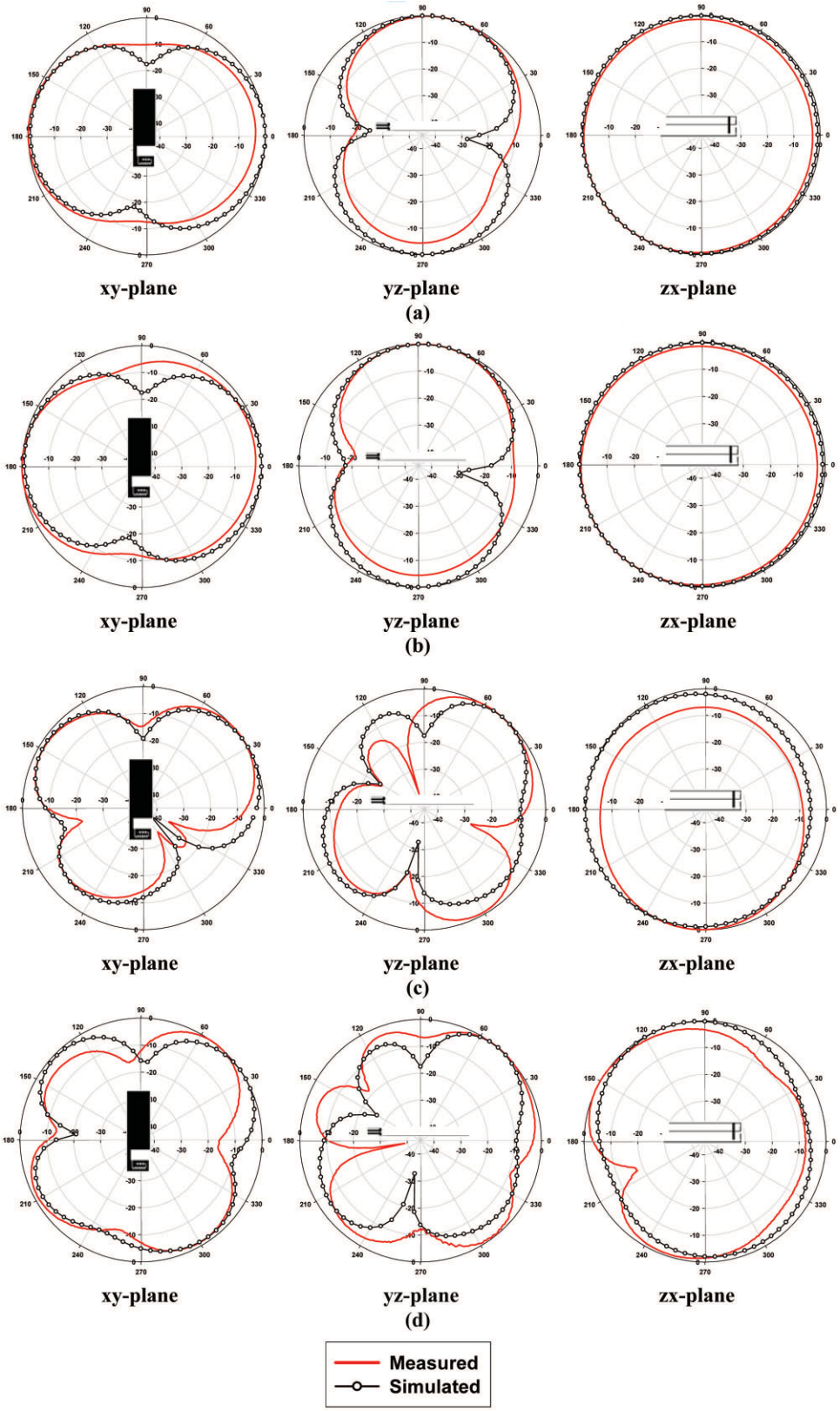

Figure 3 Radiation patterns at (a) 900 MHz, (b) 940 MHz, (c) 1860 MHz, and (d) 2400 MHz. [Color figure can be viewed in the online issue, which is available at www.interscience.wiley.com]

parallel shorting plates as shown in Figure 1(d) in an appropriate value.

3. SIMULATION AND EXPERIMENTAL RESULTS

Figure 2 describes the return losses obtained from two commercially available softwares, CST MWS and HFSS [5, 6], and measurements, resulting in similar characteristics among them with three resonant frequencies. Under the criterion of VSWR less than 2.5:1, the measured impedance bandwidths of the proposed antenna cover ~300 MHz in the lower frequency band (from 810 to 1100 MHz) and 760 MHz in the upper frequency band (from 1685 to 2445 MHz), respectively.

The radiation patterns in xy, yz, and xz plane as shown in Figure 3 indicate that the comparison between the measured data and the simulated results gives a good agreement.

From Figure 4, it is seen that the measured gains from 800 to 2400 MHz are in between the minimum 0.04 dB and the maximum 4.61 dB.

4. PARAMETRIC STUDIES

Consider the rectangular ground plane with removed area as shown in Figure 1. From Figure 5, it is estimated that the return loss of the proposed antenna is mainly dependent on the dimension of the removed area (g5 × g6) of the ground plane and the second resonant frequency near 2 GHz could be controlled by changing the antenna parameter g5. It is observed from marker A in Figure 5 that the frequency shift could be obtained according to the variation of parameter g5. Particularly when the antenna parameter g5 approaches to 12.7 mm, the input impedance bandwidth has been improved with considerable amounts.

In addition to the size effect of the ground plane on the antenna performances, it is seen from Figure 6 that the distance effect between two radiating patches is an important factor for the electrical performances of the proposed antenna. Inserting subpatch under the main patch with a certain distance results in the third resonant frequency near 2.4 GHz (dash-dotted line, short-dashed line, and solid line) while there are two resonant

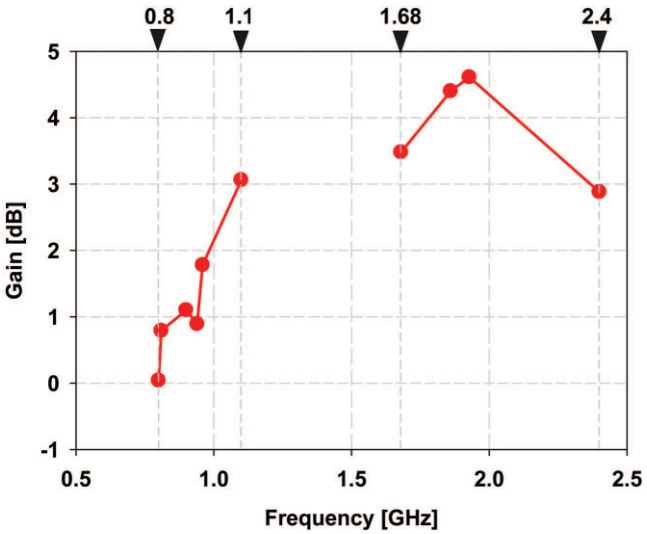

Figure 4 Measured gains at the interested frequencies. [Color figure can be viewed in the online issue, which is available at www.interscience.wiley.com]

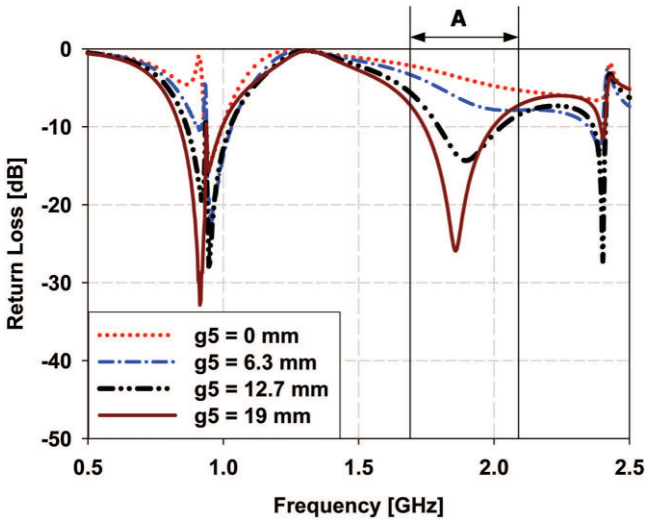

Figure 5 Return losses versus the removed area of the ground plane as a function of frequency. [Color figure can be viewed in the online issue, which is available at www.interscience.wiley.com]

frequencies near 1 and 2 GHz when only main patch exists. According to the parametric studies, it is found out that as the distance between two radiating patches becomes smaller, the input impedance bandwidth gets better at high resonant frequency.

Throughout the optimizing process related with input impedance bandwidth, effect of ground plane, and the distance between two radiating patches, the final result shows the dash-dotted line in Figure 6 at ISM band under the criterion of VSWR less than 3.

5. CONCLUSIONS

The electrical performances of a compact six-band PIFA using double and identical periodic-grooved patches with shorting plates have been investigated. In addition to that, the physical behaviors related with the resonant frequencies have been analyzed throughout the parametric studies according to the variation of the antenna structure. Also it is verified that the simulated results give reasonably good agreements with the measured data. Finally, it is guar-

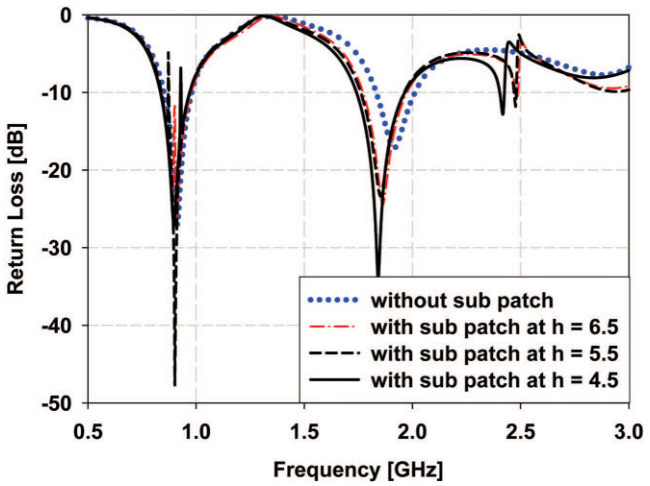

Figure 6 Return losses versus the distance between two radiating patches as a function of frequency. [Color figure can be viewed in the online issue, which is available at www.interscience.wiley.com]

anteed that the proposed antenna could be available for hand-held communication systems in terms of easy fabrication and volume reduction.

REFERENCES

1. R. Hossa, A. Byndas, and M.E. Bialkowski, Improvement of compact terminal antenna performance by incorporating open-end slots in ground plane, IEEE Microwave Wireless Compon Lett 14 (2004), 283–285.
2. H. Park, H. Jung, S. Hong, and J. Choi, An enhanced bandwidth planar inverted-F antenna with a modified shorting strip, Microwave Opt Technol Lett 49 (2007), 513–515.
3. Y.-X. Guo and G.S. Tan, New compact six-band internal antenna, IEEE Antennas Wireless Propag Lett 2 (2004), 295–297.
4. K.K. Kang, J.W. Lee, C.S. Cho, and T.K. Lee, A dual-band planar inverted-F antenna with periodic grooves, Proceedings of European Microwave Conference, Manchester, England, 2006.
5. CST Microwave Studio V5.0, 2004, Germany.
6. Ansoft High Frequency Structure Simulator V10.0, 2006, USA.

DIVIDE-BY-3 LC INJECTION LOCKED FREQUENCY DIVIDER WITH A TRANSFORMER AS AN INJECTOR'S LOAD

Sheng-Lyang Jang, Pei-Xi Lu, C. F. Lee, and M.-H. Juang
Department of Electronic Engineering, National Taiwan University of Science and Technology, 43, Keelung Road, Section 4, Taipei, Taiwan 106, Republic of China; Corresponding author: D9202209@mail.ntust.edu.tw

Received 26 February 2008

ABSTRACT: *This letter proposes a new divide-by-3 injection-locked frequency divider (ILFD) fabricated in the 0.35-μm CMOS 2P4M CMOS technology. The divider consists of a pMOS cross-coupled LC oscillator, two injection MOSFETs, and a transformer staggered in between the cross-coupled pMOSFETs and injection FETs, and the LC resonator is composed of two inductors and varactors. The injection FET uses the transformer load to increase the locking range. At the supply voltage of 2 V, the divider free-running frequency is tunable from 2.433 to 2.79 GHz, and at the incident power of 0 dBm the locking range is about 1.13 GHz (14.9%), from the incident frequency 7.17–8.3 GHz. The core power consumption is 8.64 mW. The die area is 1.36 × 0.8 mm²*. © 2008 Wiley Periodicals, Inc. Microwave Opt Technol Lett 50: 2722–2725, 2008; Published online in Wiley InterScience (www.interscience.wiley.com). DOI 10.1002/mop.23775

Key words: *0.35-μm CMOS; VCO; divide-by-3 injection-locked frequency divider; transformer; locking range*

1. INTRODUCTION

Frequency dividers (FDs) are often used in frequency synthesizers and signal generators for mixers, they take a sinusoidal input signal and generate a periodic output signal at a frequency that is a fraction of the input signal. LC tank FDs are widely used for high frequency application. FDs with odd frequency division ratios [1–6] are less common than their counterparts with even division ratios. However, they can be used with voltage-controlled oscillator (VCO) to form a frequency up- and down-conversion scheme so that the frequency pulling effect can be minimized.

The odd-modulo FD can be formed with injection-locked ring oscillators [2], which however do not provide filtering like a resonant oscillator, and hence tend to have large unwanted harmonic components, particularly at the injected signal frequency. The odd-modulo LC-tank injection-locked frequency dividers (IL-FDs) can be developed using a cross-coupled VCO with tail injection [1] or direct injection [4]. In the divide-by-3 ILFD in [1], the injection MOSFETs are in series with an nMOS cross-coupled VCO and the circuit ÷3 ILFD requires the resonant inductor load for the injection MOSFETs. In this article, a new divide-by-3 LC tank FD is proposed. The proposed circuit consists of an LC tank VCO. The two injection MOSFETs are stacked on a transformer which is in series with the cross-coupled switching transistors. The proposed ILFD uses an injection transformer load to increase the locking range instead of an inductor load [1] and was fabricated in the 0.35-μm 2P4M CMOS technology and the operational locking range of the ILFD is from the incident frequency 7.17–8.3 GHz.

2. OPERATION PRINCIPLE OF THE DIVIDE-BY-3 ILFD

Figure 1 shows the proposed CMOS divide-by-3 ILFD. The bottom part consisting of a cross-coupled pair $M1$ and $M2$ together with a resonant LC load, which consists of two inductors and two varactors connected with back to back placed in parallel with the LC resonator. Transistors $M3$ and $M4$ are V–I converters and used as injection MOSFETs. The sources of cross-coupled pair transistors are not connected to a common node but to the two output ports of a transformer and the I–V relation of an ideal transformer with inductors coupled with the transformer coupling coefficient M is described by

$$V_3 = j\omega L_3 I_3 + j\omega M I_4 \tag{1}$$

$$V_4 = j\omega L_4 I_4 + j\omega M I_3 \tag{2}$$

When the circuit is operated in the differential condition, $I_3 = -I_4$,

$$V_3 = j\omega(L_3 - M)I_3 \tag{3}$$

The transformer is used to increase the locking range. At the low fundamental frequency of ω_o, the impedance V_3/I_3 looking into the transformer from the source of $M1$ is small, while at the third-harmonic this impedance becomes large. At the oscillation frequency which in effect causes the sources of cross-coupled pair $M1$ and $M2$ be connected together at the fundamental frequency (f_o) for a large loop gain and a reliable oscillation. With no input signal, the circuit behavior is similar to a standard cross-coupled oscillator at f_o. Injectors $M3$ and $M4$ convert the differential injection voltage signals into differential drain currents, which through the transformer are converted to two source voltages of $M1$ and $M2$. Transistors $M1$ and $M2$ are no longer a differential pair at a frequency higher than f_o.

The operation principle of the ILFD shown in Figure 1 is described next, and the ILFD can be operated in the divide-by-2 and divide-by-3 mode depending on the incident frequency. First, the divide-by-3 ILFD is described. With no injection signal, the gate voltage v_g of $M1$ FET consists of frequency components with ω_o and $2\omega_o$ due to the nonlinearity of the $M1$ and $M2$. A third-degree Taylor expansion of drain current of $M1$ can be written as

$$i_{ds}^{+} = K_{3gmho2} v_s v_g^2 + \ldots \tag{4}$$

where v_s and v_g are the AC components of source voltage and gate voltage of $M1$, respectively. $K_{3\mathrm{gmho2}}$ is the cross-modulation coefficient. The source voltage v_s of $M1$ is given by